FracRisk

Reporting form for deliverables

Deliverable Number:	D6.2
Work package number:	WP6
Deliverable title	Use of electrical resistivity tomography to detect temporal near surface changes providing reliable uncertainty estimates for pollution risk assessment
Type	Report
Dissemination Level	Public
Lead participant	Dr Erica Galetti
Contributing scientists and other personnel	Prof Andrew Curtis
Schedules delivery date from DOW	30/11/2016
Actual / forecast delivery data	30/11/2016
Comments (optional)	Technical report attached

Deliverable summary text:

Hydraulic fracturing operations involve the injection of large volumes of potentially contaminating fluids into the subsurface in order to create a network of fractures through which natural gas and/or oil can be extracted from the reservoir. Hence, during such operations the near-subsurface (depths of tens to low-hundreds of metres) is potentially at risk of pollution from a number of sources, including escaping fracturing and drilling fluids, reservoir fluids migrating up the fracture network, and pollutants escaping from the drilling and production platform or the fracturing fluids storage pool.

In order to allow the near-subsurface to be monitored, and any concomitant pollution risk to be tracked over time, we have developed a new monitoring method that images the near surface using electrical resistivity tomography (ERT), which is an ideal geophysical monitoring technique in this scenario given its high sensitivity to the presence and composition of fluids in the subsurface.

The key feature of this new monitoring method is that it is fully non-linear and that, as well as providing accurate images of electrical resistivity in the subsurface, it also allows reliable and quantitative estimates of its uncertainty to be obtained for the first time. Obtaining uncertainty estimates is particularly important within a monitoring and mitigation programme as these quantities must be considered when assessing risk (i.e., if what looks like a leak from a storage pond is visible in a subsurface resistivity image, we need to know the uncertainty associated with that image to make sure that what we see is an actual leak rather than an artefact or the result of noisy data). However, reliable estimates of uncertainty have been unavailable to-date since they cannot be obtained using any currently available, traditional ERT method.

The technique developed within this deliverable therefore provide a potentially effective method for the monitoring of fluids in the subsurface and provides information that can be used within a risk assessment and mitigation programme. This is particularly important within the context of hydraulic fracturing operations given the highly contaminating nature of fracturing fluids, the poor

conditions that these fluids are normally stored in (i.e., open-air ponds on the ground surface), the potential for contamination of underground aquifers, and the fact that subsurface and aquifer contamination by fracking fluids has received particular attention by the public.

The theory associated with the method and an example of its application may be found in the attached report.

Submitted	28/11/2016
Reviewed	29/11/2016
Final submission	30/11/2016

Transdimensional Monte Carlo electrical resistivity tomography

Erica Galetti, Andrew Curtis

University of Edinburgh, School of GeoSciences
James Hutton Road, Edinburgh EH9 3FE
United Kingdom

The ability to accurately assess and estimate the uncertainty of the solution to an inverse problem is an important aspect of geophysical inversion. Within this report, we present a stochastic inversion method for electrical resistivity tomography (ERT) which makes use of Bayesian theory, the reversible-jump Markov chain Monte Carlo algorithm, and model parameterisation with Voronoi cells, to produce an ensemble of valid solutions which are distributed according to the posterior probability density function. By solving the forward problem at each Markov chain iteration and allowing the model cells to vary in number, shape and size throughout the inversion, we ensure that the physics of the forward problem is never linearised, and hence that any parametrisation- and modelling-related bias is naturally reduced to a minimum. In addition, being fully non-linear, this method provides an accurate representation of subsurface resistivity structures as well as a measure of their associated uncertainties. Within this report, we introduce the theory and method behind our inversion algorithm and present an example of its application to a synthetic dataset. We also benchmark our results by comparing them to those obtained from a more traditional, iterated-linearised inversion scheme.

1 Introduction

In recent decades, electrical resistivity tomography (ERT) methods have provided effective and non-invasive geophysical monitoring tools for the near-surface. Thanks to the sensitivity of electrical resistivity to fluid content and composition, ERT is particularly suitable for monitoring scenarios which involve the presence of fluids in the subsurface, and has been successfully applied to trace contaminants (Daily & Ramirez, 1995; Sainato et al., 2012; Auken et al., 2014), to study potential flow paths (Singha & Gorelick, 2005; Slater et al., 2002), and to detect leaks from buried pipes (Jordana et al., 2001) and storage tanks (Daily et al., 2004).

In ERT, electrical currents are actively injected into the ground from one or more electrodes, and the resulting electrical potential is measured as the potential difference between other pairs of electrodes located on or within the Earth's surface. These measurements constitute a set of observations $\mathbf{d}^{obs}$, and are used to recover the resistivity structure of the subsurface through inversion. Mathematically speaking, this involves inferring a set of model parameters $\mathbf{m}$ from the set of observed data $\mathbf{d}^{obs}$, and is achieved by solving an expression such as $\mathbf{d}^{obs} = \mathbf{g}(\mathbf{m})$ – where $\mathbf{g}$ is a function that relates $\mathbf{m}$ to $\mathbf{d}$.

However, solving an inverse problem in geophysics poses a number of challenges which go beyond merely finding a solution $\mathbf{m}$ that mathematically fits the observations. Sources of uncertainty in the solution include (but are not limited to) the presence of noise in the acquired data, limited resolution, and simplifications in the physics of the forward problem due to insufficient computing power. In addition, the inverse problem is often ill-posed, so that more than one model may adequately fit the observations. Given that these issues are unavoidable, solutions are subject to a degree of uncertainty which must be accounted for correctly. Hence, the use of stochastic (e.g., Tarantola (2005)) rather than optimisation (e.g., Parker (1994)) inversion methods is particularly beneficial since an estimate of model uncertainty can be evaluated directly from the posterior probability density function (PDF) of each model parameter.

This report presents a stochastic inversion method for resistivity tomography which uses Bayesian theory (Bayes & Price, 1763), the reversible-jump Markov chain Monte Carlo algorithm (rj-McMC – Green (1995)), and model parameterisation with Voronoi cells (Bodin & Sambridge, 2009) to solve the inverse problem of ERT and to produce an ensemble of valid solutions which are distributed according to the posterior PDF. This method can be referred to as 'transdimensional' in that the dimensionality of the model space is allowed to change across Markov chain iterations, making the number of model parameters one of the unknown quantities inverted for by the method. The main advantage of this approach lies in the fact that, by allowing the model parameters (i.e., Voronoi cells) to vary in number, shape and size, the space of possible a priori parameterisations is broadened, ensuring a more comprehensive estimation of the a posteriori uncertainty since this becomes independent of any particular choice of model parameterisation. In addition, thanks to the 'natural parsimony' of Bayesian inference, posterior models are only as complex as required by the data or by prior information: among models that provide equal fit to the observations, simpler ones (i.e., those having fewer Voronoi cells) are assigned a higher probability.

2 Method

Within a Bayesian framework, information is represented by probability density functions (PDFs). Bayesian inference makes use of Bayes' theorem (Bayes & Price, 1763) to estimate the *a posteriori* PDF $p(\mathbf{m}|\mathbf{d}^{obs})$ (defined as the probability density of model $\mathbf{m}$ given data $\mathbf{d}^{obs}$) by combining observations with *a priori* information on the model according to

$$p(\mathbf{m}|\mathbf{d}^{obs}) \propto p(\mathbf{d}^{obs}|\mathbf{m})p(\mathbf{m}) \tag{1}$$

where $\propto$ denotes proportionality, $p(\mathbf{d}^{obs}|\mathbf{m})$ is the likelihood function expressing the probability of observing dataset $\mathbf{d}^{obs}$ given model $\mathbf{m}$, and $p(\mathbf{m})$ is the *a priori* probability density representing prior information on model $\mathbf{m}$ (i.e., what we know about $\mathbf{m}$ before performing the inversion). Hence, equation (1) represents how prior information on the model is updated by the data to give the posterior distribution. Since the posterior PDF cannot normally be expressed in analytic form, it is usually evaluated numerically at different positions in the model space using McMC samplers such as the Metropolis-Hastings (MH) algorithm (Hastings, 1970). This algorithm allows an ensemble of samples (i.e., models of subsurface resistivity in this case) that fit the observed data to be produced by iteratively perturbing an initial model.

The flow diagram for our inversion algorithm is shown in Figure 1. A resistivity model $\mathbf{m}$ is defined over a Voronoi tessellation of the xz plane. The number of Voronoi cells in the model, their location and resistivity, and data noise parameters, are drawn randomly from a uniform prior distribution. At each step of the Markov chain, a new model $\mathbf{m}'$ is proposed as a perturbation of the current model by randomly choosing between five types of model perturbations (i.e., Markov chain steps): a *birth* step adds a Voronoi cell at a random location in the model; a *death* step deletes a randomly-chosen Voronoi cell; a *move* step randomly changes the location of a randomly-chosen Voronoi cell; a *resistivity* step perturbs the resistivity of a randomly-chosen Voronoi cell; a *noise* step perturbs a data noise parameter. The proposed model $\mathbf{m}'$ is either accepted or rejected depending on the value of the acceptance ratio $\alpha(\mathbf{m}'|\mathbf{m})$:

$$\alpha(\mathbf{m}'|\mathbf{m}) = \min\left[1, \frac{p(\mathbf{m}')}{p(\mathbf{m})} \times \frac{p(\mathbf{d}^{obs}|\mathbf{m}')}{p(\mathbf{d}^{obs}|\mathbf{m})} \times \frac{q(\mathbf{m}|\mathbf{m}')}{q(\mathbf{m}'|\mathbf{m})} \times |\mathbf{J}|\right] \tag{2}$$

where the second term in the square bracket involves the product of the prior ratio ($\frac{p(\mathbf{m}')}{p(\mathbf{m})}$), the likelihood ratio ($\frac{p(\mathbf{d}^{obs}|\mathbf{m}')}{p(\mathbf{d}^{obs}|\mathbf{m})}$), the proposal ratio ($\frac{q(\mathbf{m}|\mathbf{m}')}{q(\mathbf{m}'|\mathbf{m})}$), and the Jacobian ($|\mathbf{J}|$) of the transformation from $\mathbf{m}$ to $\mathbf{m}'$ (see Bodin & Sambridge (2009) for a detailed description of the terms in equation (2)).

At the end of the chain, an ensemble of representative samples is obtained by discarding the first few hundred thousand iterations from the Markov chain as 'burn-in' and only retaining one model every few tens or hundreds of iterations to ensure that the samples in the ensemble are approximately uncorrelated. Therefore,

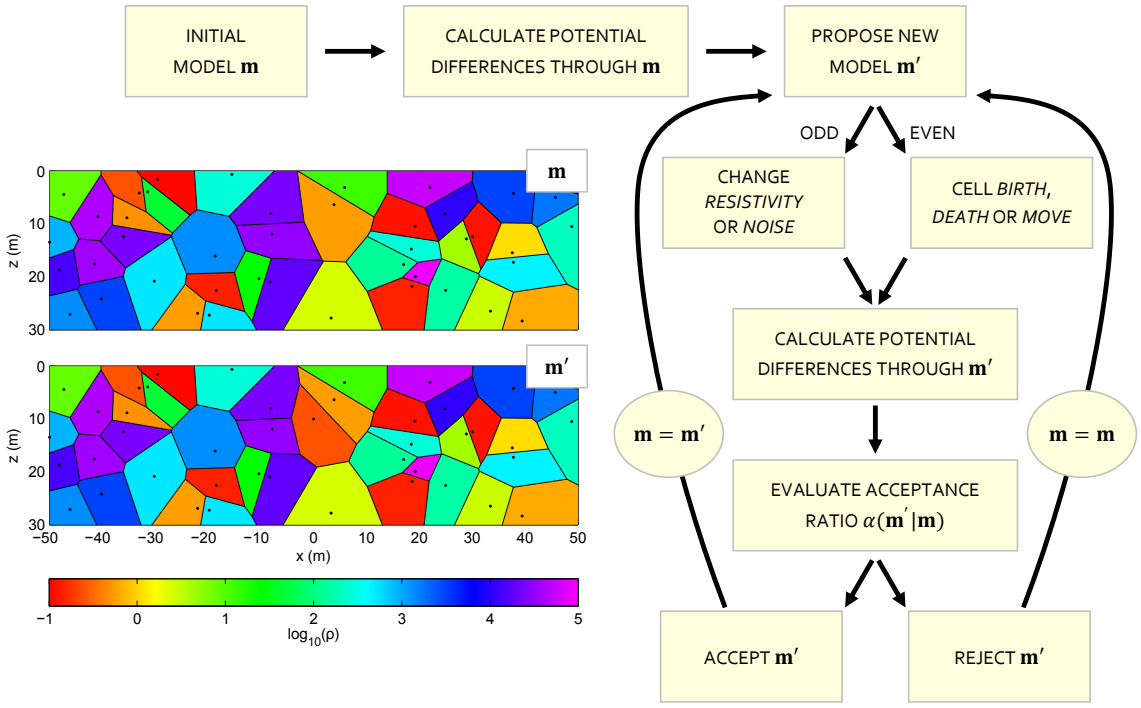

Figure 1. Workflow of the transdimensional electrical resistivity tomography (TERT) method. This samples the posterior PDF by producing an ensemble of Voronoi-tessellated models of subsurface resistivity using the rj-McMC algorithm. Each Voronoi cell is defined by the location of its nucleus (the black dots in $\mathbf{m}$ and $\mathbf{m}'$) and a value of resistivity ($\log_{10}(\rho)$). A (Markov) chain of models is obtained by following the black arrows: a new model $\mathbf{m}'$ is first proposed by modifying the current model $\mathbf{m}$, and subsequently accepted or rejected depending on its likelihood. The chain of accepted models is therefore created by repeating this step for many iterations. In this example, the geometry of model $\mathbf{m}$ is perturbed in a 'birth' step by adding a Voronoi nucleus at [0 10] m.

rather than providing a single best-fitting solution, the result of this algorithm is an ensemble of thousands of samples: although each Voronoi-tessellated model is unrealistic when taken by itself, it represents a sample from the posterior PDF, and the *whole* ensemble of models represents the solution to the inverse problem. Useful statistical moments can then be calculated from the ensemble, including low-order statistics such as an average model and an estimate of its uncertainty (e.g., standard deviation), and higher-order statistical moments such as skewness and kurtosis. In addition, by computing potential differences at each Markov chain iteration, we ensure that the physics of the forward problem is never linearised while finding an inverse problem solution.

3 Synthetic example

In order to test the effectiveness of the transdimensional electrical resistivity tomography (TERT) method, we created a synthetic dataset for the resistivity model shown in Figure 2(a). Using a Wenner configuration with 41 electrodes, we modelled 260 potential differences for different combinations of current and potential electrodes with a minimum and a maximum electrode spacing of 2 and 26 m, respectively. In order to emulate real-life scenarios where measurements are contaminated by noise, we perturbed each computed potential difference by applying random Gaussian noise with a standard deviation of 4%. The apparent resistivity section is shown in Figure 2(b).

The data was inverted using the TERT algorithm together with parallel tempering (Sambridge, 2014) in order to speed up convergence. For this example, twenty-four Markov chains were run in parallel for 500×10^3 iterations, and every 50^{th} sample after a burn-in period of 150×10^3 iterations was considered as a representative model from the posterior PDF. Figures 2(c) and (d) show the average and standard deviation of the ensemble of resistivity models. The background resistivity and the high-resistivity structure in the centre of the model

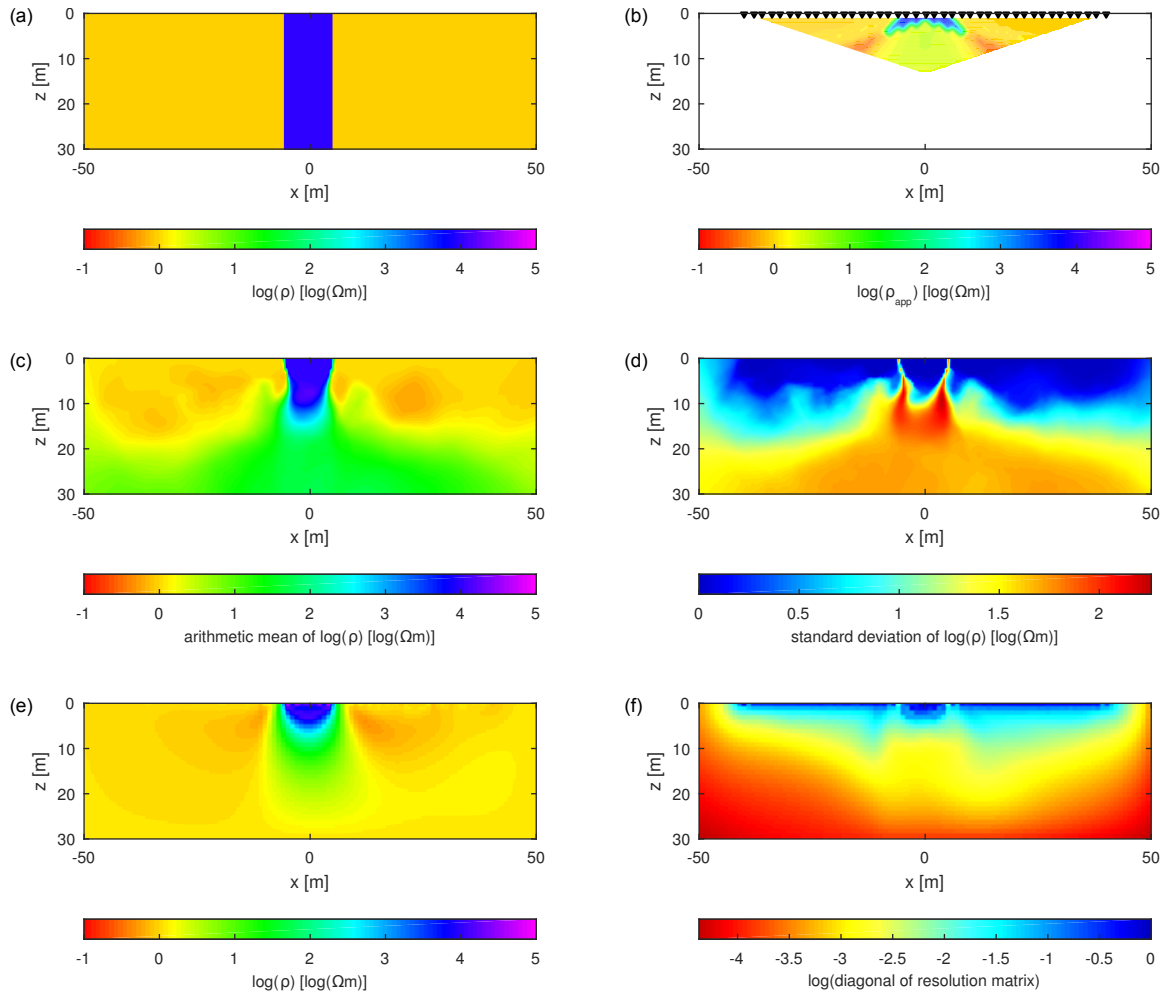

Figure 2. Synthetic ERT example. (a) True resistivity model. (b) Apparent resistivity section recorded using a Wenner configuration and the 41 electrodes indicated by the black triangles. (c) Average resistivity section from TERT. (d) Standard deviation (i.e., uncertainty) section from TERT. (e) Best-fit resistivity section from *R2*. (f) Resolution section from *R2*.

are correctly resolved down to a depth of ~ 10 m, while the lateral resolution drops beyond 40 m distance from the centre of the model in each direction. This is consistent with the resolution expected from the electrode geometry employed and can also be observed as an increase in standard deviation in panel (d). However, the standard deviation map also shows high uncertainty along the vertical boundary of the high-resistivity structure, showing that the size and shape of the anomaly cannot be constrained exactly, indeed defining precisely the spatial resolution of this boundary. The presence of this feature is independent of the electrode geometry employed, and occurs as a consequence of the true resistivity structure of the subsurface. Similar features called 'uncertainty loops' have been observed in non-linear seismic traveltime tomography (Galetti et al., 2015), but have not been observed in electrical resistivity tomography to the best of our knowledge.

In order to benchmark the TERT algorithm, we inverted the same dataset using the iterative linearised code *R2* by Binley (2016). The resulting resistivity model is shown in Figure 2(e), while panel (f) displays the diagonal elements of the resolution matrix (e.g., see equation (5.18) in Binley & Kemna (2005)). While the resistivity model in panel (e) is relatively similar to the average model in (c) within the resolved area, the resolution map in (f) appears to be mainly influenced by the electrode geometry, and hence does not provide any indication of the true uncertainty of the structures observed in (e). In addition, by correctly accounting for the non-linearity of the inverse problem in TERT, structures in (c) are resolved to almost twice the depth compared to those in (e) from linearised inversion.

4 Conclusions

The ability to accurately estimate the uncertainty of the solution to an inverse problem is an important requirement in geophysics. Within this report, we presented an inversion method which makes use of the rj-McMC algorithm and variable model parameterisation with Voronoi cells to invert potential differences in a transdimensional electrical resistivity tomography scheme. Besides yielding an accurate representation of the subsurface resistivity structure, this method provides a measure of the uncertainty of the resolved structures. In addition, because the model parameterisation is allowed to vary throughout the inversion and the forward problem is solved at each Markov chain iteration, parameterisation- and modelling-related biased are naturally minimised.

5 Acknowledgements

We thank T. Bodin and M. Sambridge for many discussions on transdimensional inversion methods. Forward modelling for the synthetic example presented and within our Matlab TERT code was performed using the *FW2_5D* package by Pidlisecky & Knight (2008).

References

Auken, E., Doetsch, J., Fiandaca, G., Christiansen, A. V., Gazoty, A., Cahill, A. G., & Jakobsen, R., 2014. Imaging subsurface migration of dissolved CO2 in a shallow aquifer using 3-D time-lapse electrical resistivity tomography, *Journal of Applied Geophysics*, **101**, 31–41.

Bayes, M. & Price, M., 1763. An Essay towards Solving a Problem in the Doctrine of Chances. By the Late Rev. Mr. Bayes, F. R. S. Communicated by Mr. Price, in a Letter to John Canton, A. M. F. R. S., *Philosophical Transactions*, **53**, 370–418.

Binley, A., 2016. *R2 version 3.0 (March 2016)*, University of Lancaster.

Binley, A. & Kemna, A., 2005. DC Resistivity and Induced Polarization Methods, in *Hydrogeophysics*, pp. 129–156, eds Rubin, Y. & Hubbard, S. S., Springer, Dordrecht, Netherlands.

Bodin, T. & Sambridge, M., 2009. Seismic tomography with the reversible jump algorithm, *Geophysical Journal International*, **178**(3), 1411–1436.

Daily, W. & Ramirez, A., 1995. Electrical resistance tomography during in-situ trichloroethylene remediation at the Savannah River Site, *Journal of Applied Geophysics*, **33**(4), 239–249.

Daily, W., Ramirez, A., & Binley, A., 2004. Remote Monitoring of Leaks in Storage Tanks using Electrical Resistance Tomography: Application at the Hanford Site, *Journal of Environmental and Engineering Geophysics*, **9**(1), 11–24.

Galetti, E., Curtis, A., Meles, G. A., & Baptie, B., 2015. Uncertainty loops in travel-time tomography from nonlinear wave physics, *Physical Review Letters*, **114**(14), 148501.

Green, P. J., 1995. Reversible jump Markov chain Monte Carlo computation and Bayesian model determination, *Biometrika*, **82**(4), 711–732.

Hastings, W. K., 1970. Monte Carlo sampling methods using Markov chains and their applications, *Biometrika*, **57**(1), 97–109.

Jordana, J., Gasulla, M., & Pallàs-Areny, R., 2001. Electrical resistance tomography to detect leaks from buried pipes, *Measurement Science and Technology*, **12**(8), 1061–1068.

Parker, R. L., 1994. *Geophysical Inverse Theory*, Princeton University Press.

Pidlisecky, A. & Knight, R., 2008. FW2_5D: A MATLAB 2.5-D electrical resistivity modeling code, *Computers & Geosciences*, **34**(12), 1645–1654.

Sainato, C. M., Losinno, B. N., & Malleville, H. J., 2012. Assessment of contamination by intensive cattle activity through electrical resistivity tomography, *Journal of Applied Geophysics*, **76**, 82–91.

Sambridge, M., 2014. A Parallel Tempering algorithm for probabilistic sampling and multimodal optimization, *Geophysical Journal International*, **196**(1), 357–374.

Singha, K. & Gorelick, S. M., 2005. Saline tracer visualized with three-dimensional electrical resistivity tomography: Field-scale spatial moment analysis, *Water Resources Research*, **41**(5), W05023.

Slater, L., Binley, A., Versteeg, R., Cassiani, G., Birken, R., & Sandberg, S., 2002. A 3D ERT study of solute transport in a large experimental tank, *Journal of Applied Geophysics*, **49**(4), 211–229.

Tarantola, A., 2005. *Inverse Problem Theory and Methods for Model Parameter Estimation*, SIAM.